Elasto-geometrical Calibration of an Industrial Robot under Multidirectional External Loads Using a Laser Tracker*

Kaveh Kamali, Ahmed Joubair, Ilian A. Bonev, Pascal Bigras

Abstract— **This paper presents an elasto-geometrical calibration method for improving the position accuracy of an industrial robot (ABB IRB 1600). Geometric parameter errors and joint stiffness parameters are identified through measuring the position of the robot's end-effector in several robot configurations using a laser tracker. Contrary to previous works, robot's position errors are measured under a wide range of external forces and torques for each robot configuration. A 6-DOF cable-driven parallel robot is employed to automatically apply the desired load on the end-effector of the ABB robot. Before the experiment, an observability analysis is performed in order to improve the robustness of the calibration process with respect to measurement noise and unmodeled errors. Accordingly, an optimal set of robot configurations and external loads is selected for the calibration process. The measured position errors of the ABB robot for this selected set are used to identify the real robot's elasto-geometrical parameters. Finally, the calibration efficiency is evaluated for a number of random combinations of robot configurations and external loads. The experimental results revealed that the proposed elasto-geometrical calibration approach is able to reduce the maximum position error to 0.960 mm, while a customary kinematic calibration can reduce the maximum position error only to 2.571 mm.**

I. Introduction

Nowadays there is a growing demand for industrial robots with higher accuracy. Most of the current industrial robots have a great repeatability, but their accuracy is poor. As long as a robot has good repeatability, the robot's accuracy can be improved through a process called calibration. Current research works in robot calibration can be classified into three levels of calibration [1, 2]: level-1 (also called mastering), which only models the joint errors; level-2 [3–5], which deals with the kinematic model inaccuracies; and level-3, (also called "non-kinematic calibration"), which models errors other than geometric ones, such as joint elasticity, thermal distortion and expansion of robot parts, friction, joint clearance, and link flexibility [6, 7]. Joint elasticity in industrial serial robots is an important non-kinematic source of errors, which is caused by static and dynamic loads. For low-speed applications such as riveting, drilling or fiber placement, dynamic loads can be ignored. Static loads include gravitational and external loads. When high volumetric accuracy is desired, joint elasticity errors play an important role, especially in the presence of varying external loads.

Several basic works were carried out for measurement of joint deflections of serial robots under external loads. Wu et al. [8] proposed a methodology for joint stiffness identification of industrial serial robots. They applied external forces on a robot using a mass connected to the end-effector by means of a chain and a spring balance. Marie et al. [9] utilized a cable-pulley system with deadweights in order to apply force to the robot end-effector. In another study, Wang et al. [10] applied external forces by an air cylinder through a pulley relayed string. Another approach is to measure the flexibility of the robot only under the effect of gravitational forces. Joubair et al. [11] performed non-kinematic calibration of a FANUC LR Mate 200iC industrial robot. In their calibration model, the gravity effect of the robot structure is taken into account. In yet another study, Nubiola and Bonev [12] improved the absolute accuracy of an ABB IRB 1600 industrial robot. Rather than relying solely on gravitational forces, the authors also used different payloads in order to more accurately identify the stiffness model of the robot.

In all of the above-mentioned works, the focus was on only gravitational forces and/or external forces which are usually applied in one direction (e.g., pulling the end-effector with a single cable). To the best of our knowledge, the effect of a wide range of multidirectional external loads (forces and torques) in various directions has never been studied before. Furthermore, most of the previous works rely on manual mechanisms for imposing load on the robot tool. These methods are time-consuming, potentially hazardous, and make it complicated to measure the position error of the robot for a large number of external loads and robot configurations.

In this study, we present a new experimental setup for calibration of an ABB IRB 1600-6/1.45 industrial serial robot under a wide range of multidirectional external loads. This calibration is achieved inside a specific target workspace (500 mm × 500 mm × 500 mm). An elasto-geometrical model of the end-effector position is used in the calibration process which models kinematics and joint flexibilities of the robot. The effect of other non-kinematic errors (e.g. thermal and backlash errors) are not considered in this model. The calibration aims to identify the real kinematic and joint flexibility parameters. To this end, position of the ABB robot end-effector is measured in different robot configurations and under different external loads, using a laser tracker. Next, the model parameters are identified via an optimization process.

A six degree-of-freedom (DOF) cable-driven parallel robot is designed and constructed to automatically apply multidirectional external wrenches (forces and torques) on the end-effector of the serial robot. To do so, the moving platform of the cable-driven robot is attached to the flange of the serial robot through a 6-axis force/torque sensor. A force controller is used to apply the desired wrench on the moving platform

*Research supported by Canada Research Chairs. The authors are with the École de technologie supérieure (e-mail: ilian.bonev@etsmtl.ca).

of the cable-driven robot. The force/torque sensor measures the exact wrench imposed on the robot flange.

Cable-driven robots are a type of parallel robots in which the moving platform is connected to the base through actuated cables [13]. These robots have several interesting features such as high payload-to-weight ratio, large and extendable workspace, simple structure and ease of reconfiguration. They are also able to exert a vast range of wrenches on their moving platform with good accuracy. Therefore, a cable-driven robot is a suitable system to apply multidirectional external loads on the end-effector of the industrial robot.

The contributions of this study are: (1) we used a novel experimental setup based on a 6-DOF cable-driven robot to apply a wide range of multidirectional wrenches on the end-effector of the serial robot during the calibration process; (2) we performed an observability analysis not only on a set of possible robot configurations but also on the variation of direction and magnitude of the external wrenches applied to the robot end-effector (i.e., we selected the robot configurations and external wrenches used for parameter identification based on an observability analysis); (3) we developed a fully automated process for measuring the position of the robot end-effector and the exact wrench applied, for various robot configurations and external loads.

The remainder of this paper is organized as follows: in Section 2, the calibration model (including the kinematic parameters and joint flexibilities) is developed. The process of parameter identification based on a linearized model is presented in Section 3. Section 4 describes the experiment design. In this section, an observability analysis is carried out in order to select an optimal calibration set (i.e., robot configurations and wrenches). In the next section, the experimental setup and measurement procedure are illustrated. The experimental results are presented and discussed in Section 6. Finally, conclusions are given in Section 7.

II. Robot Calibration Model

This paper describes an elasto-geometrical calibration of a six-DOF serial robot (ABB IRB 1600-6/1.45) in order to identify and compensate its position errors in the presence of external wrenches applied to the robot end-effector. As illustrated in Fig. 1, a six-DOF cable-driven parallel robot is used to apply the desired wrench on the end-effector of the serial robot. The moving platform of the cable-driven robot is attached to the serial robot's flange (Fig. 1); therefore, the cable-driven robot is able to impose any desired wrench (limited to its wrench-feasible workspace) on the flange of the serial robot. A FARO laser tracker measures the exact position of the robot's end-effector. The measured coordinates are used for identification of the calibration model parameters.

An important step of the calibration process is choosing the appropriate calibration model that describes the position of the robot end-effector as a function of the robot parameters. Here the calibration model includes both the direct kinematics and a stiffness model (i.e., the kinematic and joint stiffness parameters of the robot). We start by describing the reference frames used in our model.

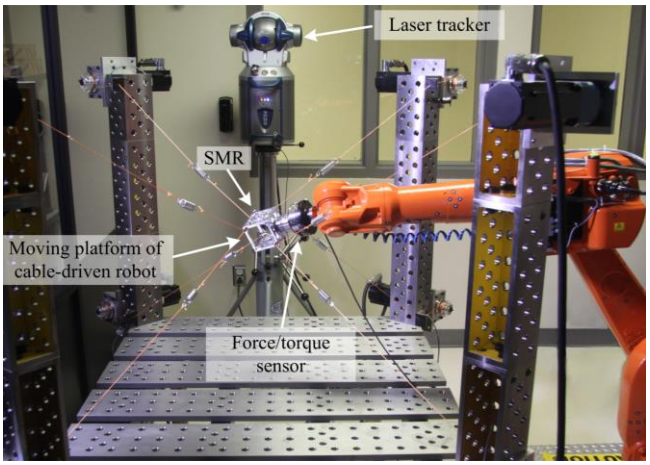

Figure 1. Experimental setup for elasto-geometrical calibration process of the ABB IRB 1600-6/1.45 robot

A. Reference Frames Description

The serial robot consists of six revolute joints and six links. Based on the Modified Denavit-Hartenberg (MDH) approach [14], seven reference frames are assigned to the robot: the base reference frame (F_0) and six frames assigned to the joints ($F_1, F_2, \ldots, F_6$), as shown in Fig. 2. Additionally, two reference frames, F_{tool} and F_{world}, are assigned to the robot's end-effector and the laser tracker, respectively.

The moving platform of the cable-driven robot is considered as a part of the ABB robot tool because it is rigidly attached to the ABB robot flange through a force/torque sensor and a tool changer. The laser tracker target (SMR) is at the origin of the tool frame F_{tool} on the robot end-effector; therefore, the measured coordinates by the laser tracker represent a translation of the tool frame F_{tool} with respect to (w.r.t.) the world frame F_{world}.

B. Kinematic Model

The MDH approach is deployed to model the kinematics of the serial robot. Given the joint angular position vector $\boldsymbol{\theta} = [\theta_1, \theta_1, \cdots, \theta_6]^{\mathrm{T}}$ as the input, the direct kinematic model is represented as

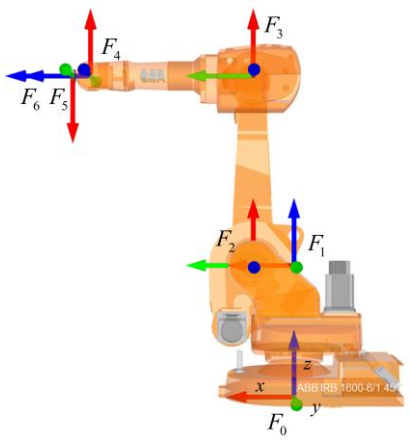

Figure 2. Frame assignment for the serial robot

$$\mathbf{H}(\boldsymbol{\theta}) = \mathbf{A}_0^{\text{world}}\mathbf{A}_1^0\mathbf{A}_2^1\mathbf{A}_3^2\mathbf{A}_4^3\mathbf{A}_5^4\mathbf{A}_6^5\mathbf{A}_{\text{tool}}^6 \ , \tag{1}$$

where $\mathbf{A}_{\text{tool}}^6$ is the homogenous transformation matrix from the F_{tool} frame to the F_6 frame, and $\mathbf{A}_0^{\text{world}}$ is the transformation matrix from F_0 to F_{world}. For $0 < i \le 6$, $\mathbf{A}_i^{i-1}$ is the transformation matrix of F_i to F_{i-1}. Using MDH parameters, matrix $\mathbf{A}_i^{i-1}$ is obtained as

$$\mathbf{A}_i^{i-1} = Rot(x,\alpha_i)Trans(a_i,\ 0,\ 0)Rot(z,\theta_i)Trans(0,\ 0,\ d_i)\ , \tag{2}$$

where α_i, θ_i, a_i and d_i are the MDH parameters of the ABB serial robot. The transformation matrices $\mathbf{A}_{\text{tool}}^6$ and $\mathbf{A}_0^{\text{world}}$ are defined as follows:

$$\mathbf{A}_0^{\text{world}} = Rot(x,\alpha_{\text{w}})Rot(y,\beta_{\text{w}})Rot(z,\gamma_{\text{w}})Trans(x_{\text{w}},y_{\text{w}},z_{\text{w}}), \tag{3}$$

$$\mathbf{A}_{\text{tool}}^6 = Rot(x,\ \alpha_{\text{t}})Rot(y,\ \beta_{\text{t}})Rot(z,\ \gamma_{\text{t}})Trans(x_{\text{t}},\ y_{\text{t}},\ z_{\text{t}})\ , \tag{4}$$

where $(x_{\text{w}}, y_{\text{w}}, z_{\text{w}})$ is the translation and $(\alpha_{\text{w}}, \beta_{\text{w}}, \gamma_{\text{w}})$ is the orientation (described in XYZ fixed Euler angles) of the base frame w.r.t. the world frame. Moreover, $(x_{\text{t}}, y_{\text{t}}, z_{\text{t}})$ and $(\alpha_{\text{t}}, \beta_{\text{t}}, \gamma_{\text{t}})$ are the position and orientation of the tool frame with respect to the reference frame F_6.

In our calibration process, we only measure the position of the robot end-effector; therefore, the direct kinematics of the robot can be expressed as

$$\begin{bmatrix}\mathbf{x}\\ 1\end{bmatrix} = \mathbf{A}_{\text{tool}}^{\text{world}}\begin{bmatrix}0 & 0 & 0 & 1\end{bmatrix}^{\text{T}}, \tag{5}$$

where $\mathbf{x}$ is the position of the end-effector w.r.t. the world reference frame F_{world}.

C. Stiffness Model

In order to include the joint compliance in the error model, an elasticity model of all the ABB robot joints is developed. Considering that the deformations are fairly small, each joint is modeled as a linear torsional spring. Therefore, compliance of the i^{th} joint can be represented by a constant compliance coefficient k_i and its rotational deflection $\tilde{\theta}_i$ is modeled by the following equation:

$$\tilde{\theta}_i = k_i\tau_i\ , \tag{6}$$

where τ_i is the torque supported by the i^{th} joint. In our model, only static loads are considered. As it can be seen in Fig. 3, the external force and torque on the robot end-effector, and the gravitational forces on each robot link are considered as the sources of static torque on each joint. The gravity vector w.r.t. the reference frame F_i can be obtained by

$$\begin{bmatrix}\mathbf{g}_i\\ 0\end{bmatrix} = \left(\mathbf{A}_i^0\right)^{\text{T}}\begin{bmatrix}\mathbf{g}_0\\ 0\end{bmatrix}, \tag{7}$$

where $\mathbf{g}_0 = \begin{bmatrix}0 & 0 & -9.81\end{bmatrix}^{\text{T}}$ is the gravitational acceleration vector, and $\mathbf{A}_i^0$ is the transformation matrix from the reference frame F_i to the base frame F_0. The following general relation is used to calculate the $\mathbf{A}_j^i$ matrix:

$$\mathbf{A}_j^i = \mathbf{A}_{i+1}^i\cdots\mathbf{A}_{j-1}^{j-2}\mathbf{A}_j^{j-1}. \tag{8}$$

Defining $\mathbf{f}_j^i$ as the gravitational force on link j w.r.t. frame F_i and $\mathbf{c}_j^i$ as the center of gravity of link j w.r.t. F_i, we have:

$$\mathbf{f}_j^i = m_j\mathbf{g}_i\ , \tag{9}$$

$$\begin{bmatrix}\mathbf{c}_j^i\\ 1\end{bmatrix} = \mathbf{A}_j^i\begin{bmatrix}\mathbf{c}_j\\ 1\end{bmatrix}, \tag{10}$$

where m_j is the mass and $\mathbf{c}_j = \begin{bmatrix}c_{\text{x},j}, c_{\text{y},j}, c_{\text{z},j}\end{bmatrix}^{\text{T}}$ is the center of gravity of link j w.r.t. F_j. Therefore, the torque generated by the gravitational force on link j on the axis of joint i is,

$$\tau_{i,\text{link}\,j} = [0 \quad 0 \quad 1]^{\text{T}}\bullet\left(\mathbf{c}_j^i\times\mathbf{f}_j^i\right). \tag{11}$$

In this equation $(\bullet)$ and $(\times)$ indicate dot and cross products, respectively. Furthermore, the external wrench on the robot tool causes an additional static torque on each robot joint. Defining $\mathbf{p}^{\text{tool}} = \begin{bmatrix}p_{\text{x}}^{\text{tool}} & p_{\text{y}}^{\text{tool}} & p_{\text{z}}^{\text{tool}}\end{bmatrix}^{\text{T}}$ as the position of the applied force on the tool w.r.t. the tool frame, the torque generated by the external wrench on the axis of i^{th} joint can be obtained as

$$\tau_{i,\text{ext}} = [0 \quad 0 \quad 1]^{\text{T}}\bullet\left(\mathbf{p}^i\times\mathbf{f}_{\text{ext}}^i + \boldsymbol{\tau}_{\text{ext}}^i\right), \tag{12}$$

where,

$$\begin{bmatrix}\mathbf{f}_{\text{ext}}^i\\ 0\end{bmatrix} = \mathbf{A}_{\text{tool}}^i\begin{bmatrix}\mathbf{f}_{\text{ext}}^{\text{tool}}\\ 0\end{bmatrix}, \tag{13}$$

$$\begin{bmatrix}\boldsymbol{\tau}_{\text{ext}}^i\\ 0\end{bmatrix} = \mathbf{A}_{\text{tool}}^i\begin{bmatrix}\boldsymbol{\tau}_{\text{ext}}^{\text{tool}}\\ 0\end{bmatrix}, \tag{14}$$

$$\begin{bmatrix}\mathbf{p}^i\\ 1\end{bmatrix} = \mathbf{A}_{\text{tool}}^i\begin{bmatrix}\mathbf{p}^{\text{tool}}\\ 1\end{bmatrix}. \tag{15}$$

The combination of all static torques caused by external

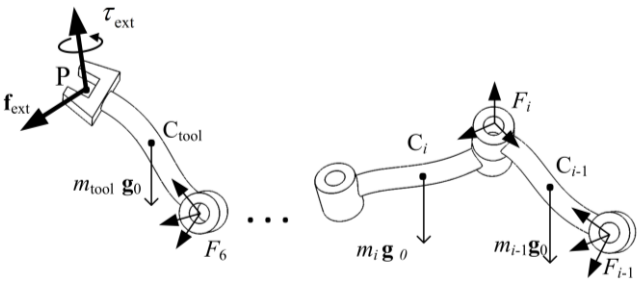

Figure 3. Schematics of the serial robot links under external load and the gravity effect

wrench and link weight supported by i^{th} joint is calculated through the following equation:

$$\tau_i = \tau_{i,ext} + \sum_{j=i}^{6} \tau_{i,\text{link}\,j} \,. \tag{16}$$

D. Elasto-geometrical Calibration Model

The elasto-geometrical calibration model comprises the kinematic calibration model and the elasticity model of all robot joints. Kinematic parameters include robot dimension errors ($\delta\alpha_i$, δa_i and δb_i), joints offsets ($\delta\theta_i$), pose (orientation and position) of the measurement device w.r.t. the robot base (x_{w}, y_{w}, z_{w}, α_{w},β_{w},γ_{w}) and robot tool pose w.r.t. the robot flange (x_{t}, y_{t},z_{t}, α_{t}, β_{t}, γ_{t}). Non-kinematic parameters are the stiffness parameters (k_i, $i = 1, \ldots, 6$). For simplification, the values of mass and center of gravity of each robot link (m_i , $\mathbf{c}_j^i$) are supposed to be known. The approximate values of mass and center of gravity for the ABB 1600/1.45 robot (provided by ABB) are used in this study. The MDH parameters including the joint stiffness and offsets are presented in Table I.

Using the MDH parameters of Table I, the direct kinematic model of (5) gives the end-effector position vector as a function of the joint rotations, external load, kinematic parameters, and joint stiffness parameters. Therefore, the estimated position of the end-effector can be expressed as,

$$\mathbf{x}_{\text{est}} = f\left(\mathbf{v}, \mathbf{q}\right) \tag{17}$$

where $\mathbf{x}_{\text{est}}$ is the estimated position of the end-effector, $\mathbf{v}$ is the vector of all the robot parameters and $\mathbf{q} = \begin{bmatrix} \boldsymbol{\theta}^{\text{T}} & \mathbf{W}^{\text{T}} \end{bmatrix}^{\text{T}}$ is the vector of joint angles ($\boldsymbol{\theta}$) and external wrench ($\mathbf{W}$) applied on the end-effector.

III. Parameter Identification

The aim of our calibration process is to find a good estimation of the real values of the robot parameters. This can be done by measuring the position of the end effector for a set of different combinations of robot configurations and external wrenches, hereafter referred to as *conf-wrench* combinations. For the k^{th} measurement, the position error is presented by

$$\Delta\mathbf{x}^k = \mathbf{x}^k_{\text{measured}} - \mathbf{x}^k_{\text{est}} \,. \tag{18}$$

TABLE I. MDH and joint stiffness parameters

i	$\alpha_i(\circ)$	$a_i(mm)$	$\theta_i(\circ)$	$d_i(mm)$
1	0	0	$\theta_1 + \delta\theta_1 + k_1\tau_1$	486.5
2	$-90+\delta\alpha_2$	$150+\delta a_2$	$\theta_2 + \delta\theta_2 + k_2\tau_2$	δd_2
3	$\delta\alpha_3$	$700+\delta a_3$	$\theta_3 - 90 + \delta\theta_3 + k_3\tau_3$	δd_3
4	$-90+\delta\alpha_4$	δa_4	$\theta_4 + \delta\theta_4 + k_4\tau_4$	$600+\delta d_4$
5	$90+\delta\alpha_5$	δa_5	$\theta_5 + \delta\theta_5 + k_5\tau_5$	δd_5
6	$-90+\delta\alpha_6$	δa_6	$\theta_6 + 180 + \delta\theta_6 + k_6\tau_6$	$65+\delta d_6$

Ideally, we want to identify the vector of robot parameters ($\mathbf{v}$) which makes the position error zero; therefore, measurement of the end-effector position for any set of joint angles ($\boldsymbol{\theta}^k$) and the vector of the external wrench ($\mathbf{W}^{\text{k}}$) yields three non-linear equations (x, y and z) as follows,

$$\mathbf{x}^k_{\text{measured}} - f\left(\mathbf{v}, \mathbf{q}^k\right) = 0 \,. \tag{19}$$

Consequently, to identify m parameters, at least $m/3$ 3D position measurements must be performed.

A. Linearization

The robot parameters can be identified by solving the set of non-linear equations of (19) for all the measurements. In order to simplify this non-linear problem, the corresponding equations are linearized around the nominal values as the initial estimation of the robot parameters. The differential form of (17) for the k^{th} measurement can be expressed as,

$$\Delta\mathbf{x}^k = \mathbf{J}^k \Delta\mathbf{v} \,, \tag{20}$$

where the Jacobian matrix $\mathbf{J}^k$ is obtained by differentiating (17) with respect to the calibration parameters as follows,

$$\mathbf{J}^k(\mathbf{v}, \mathbf{q}^k) = \left.\frac{\partial f(\mathbf{v}, \mathbf{q})}{\partial \mathbf{v}}\right|_{\mathbf{q} = \mathbf{q}^k} \,. \tag{21}$$

For a set of n measurements we have the following linear equation:

$$\Delta\mathbf{X} = \mathbf{J}\Delta\mathbf{v} \,, \tag{22}$$

where vector $\Delta\mathbf{X}$ includes all vectors of position errors of the end-effector,

$$\Delta\mathbf{X} = \begin{bmatrix} (\Delta\mathbf{x}^1)^{\text{T}} & (\Delta\mathbf{x}^2)^{\text{T}} & \cdots & (\Delta\mathbf{x}^n)^{\text{T}} \end{bmatrix}^{\text{T}} . \tag{23}$$

The identification Jacobian $\mathbf{J}$ is a $3n \times m$ matrix:

$$\mathbf{J} = \begin{bmatrix} (\mathbf{J}^1)^{\text{T}} & (\mathbf{J}^2)^{\text{T}} & \cdots & (\mathbf{J}^n)^{\text{T}} \end{bmatrix}^{\text{T}} . \tag{24}$$

B. Parameter Identification

The linearized calibration model (22) can be used iteratively to find a good estimation of the real robot parameter $\mathbf{v}_{\text{real}}$. This is done by the following procedure,

(a) Set the initial value of vector $\mathbf{v}$ equal to the nominal values ($\mathbf{v} = \mathbf{v}_{\text{nom}}$).

(b) Calculate the identification Jacobian matrix $\mathbf{J}$ for the current $\mathbf{v}$ vector.

(c) Use the current value of $\mathbf{v}$ in direct kinematics equations (17) to find the estimated position of the end-effector ($\mathbf{x}^k_{\text{est}}$) for all the selected conf-wrench combinations ($k = 1, \ldots, n$).

(d) Calculate the vector of position errors ($\Delta\mathbf{X}$) of the robot for all the measurements.

(e) Use the pseudo-inverse of $\mathbf{J}$ to estimated value of $\Delta\mathbf{v}$ as follows,

$$\Delta\mathbf{v} = \left(\mathbf{J}^{\text{T}}\mathbf{J}\right)^{-1}\mathbf{J}^{\text{T}}\Delta\mathbf{X} \tag{25}$$

(f) Add $\Delta\mathbf{v}$ to the current value of the vector $\mathbf{v}$.

(g) Repeat steps (b) to (f) until the $\|\Delta\mathbf{X}\|$ converges to a stop criteria.

The final value of $\mathbf{v}$ is the final estimation of the robot parameters.

C. Observability Index

It is important to choose an optimal set of conf-wrench combinations for the calibration. An optimal set of conf-wrench combinations makes the calibration more robust to uncertainties and measurement noise. Based on the linearized model, an observability index of the identification Jacobian can be used as an indicator of the observability of the parameter errors. Different formulations of the observability index are proposed in the literature. However, according to [15], the most appropriate index is the one introduced in [16],

$$O = \frac{\sqrt[m]{\sigma_1\sigma_2\cdots\sigma_m}}{\sqrt{n}}, \tag{26}$$

where O is the observability index, n is the number of calibration measurements, m is the number of parameters, and σ_i are the singular values of the singular value decomposition (SVD),

$$\mathbf{J} = \mathbf{U}\mathbf{\Sigma}\mathbf{V}^{\mathrm{T}}, \tag{27}$$

where $\mathbf{U}$ and $\mathbf{V}$ are orthonormal matrices and $\mathbf{\Sigma}$ is an $n \times m$ matrix as follows,

$$\mathbf{\Sigma} = \begin{bmatrix} \sigma_1 & 0 & \cdots & 0 \\ \vdots & \vdots & \vdots & \vdots \\ 0 & 0 & \cdots & \sigma_m \\ 0 & 0 & \cdots & 0 \\ \vdots & \vdots & \vdots & \vdots \\ 0 & 0 & \cdots & 0 \end{bmatrix}. \tag{28}$$

D. Identifiable Parameters

Some robot parameters are not identifiable during the calibration process. By solving (29), we can only identify the independent parameters. Some of the dependent parameters can be easily detected from the geometry of the robot. For example, the parameters d_2 and d_3 are dependent because the axes of joints 2 and 3 are parallel. The remaining dependent parameters can be detected by rank analysis of $\mathbf{J}$ around the nominal values of the robot parameters, as presented in [17]. In addition to the elimination of all the redundant parameters from the $\mathbf{v}$ vector, the corresponding columns are removed from $\mathbf{J}$ as well. In this study, the calibration model includes $m = 39$ parameters. Among them, seven dependent parameters are detected. Since the redundant parameters cannot be identified during the calibration process, we will use the nominal values of these parameters in the calibration model. It should be noted that the inaccuracy of nominal values of the redundant parameters does not affect the robot position accuracy because these errors are compensated in the corresponding redundant parameters, as stated in [6].

IV. Experiment Design

To design an optimum experimental strategy based on our measurement method and experimental conditions, we first generate a large set of different configurations and external loads. In this study, the measurements are limited to the workspace of the cable-driven robot. The dimensions of the workspace are approximately 500 mm × 500 mm × 500 mm. We discretized the workspace to 125 measurement points (5 × 5 × 5). For each point, one robot configuration is generated. Next, an observability analysis is performed to select the most appropriate set of conf-wrench combinations for the parameter identification process.

A. Generating Conf-wrench Combinations

The process of generating appropriate conf-wrench combinations for our experiment is as follows:

(a) Generating 125 poses for the end-effector of the ABB robot. The end-effector positions are uniformly distributed inside the cable-driven robot workspace while the orientations are randomly selected. However, the orientations are constrained in such a way that the SMR is always visible by the laser tracker.

(b) Solving the robot inverse kinematics, in order to calculate the joint angles for each pose obtained in step (a). When there are multiple solutions, one of them is randomly selected; however, the selected configuration should avoid collisions between the serial robot and the cable-driven robot.

(c) Generating seven random wrench vectors for each configuration. The generated forces and torques are normally distributed in the range of −120 N to 120 N and −10 Nm to 10 Nm, respectively. Furthermore, the wrenches are constrained to be in the wrench-feasible workspace of the cable-driven robot.

The above process yields 875 robot conf-wrench combinations (125 robot configurations with 7 different wrenches for each of them). Fig. 4 shows the 125 end-effector poses used for our calibration process.

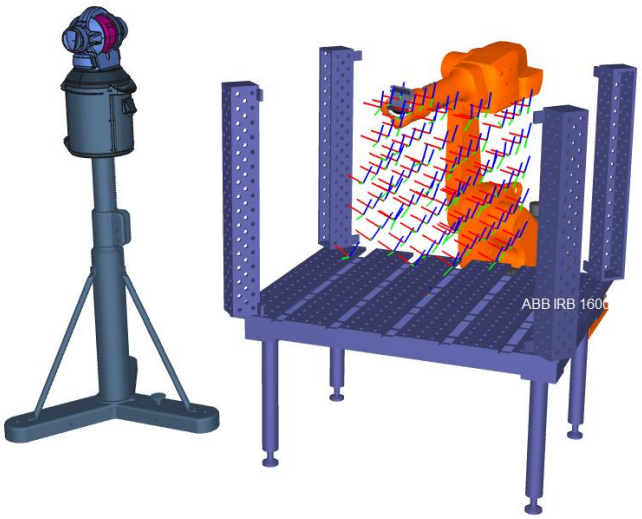

Figure 4. The 125 poses of the ABB robot end-effector which are generated inside the workspace of the cable-driven robot

B. Selection of Optimal Set of Calibration Experiments

Using the observability index, we can find the optimal set of the conf-wrench combinations dedicated to the identification process. Different approaches may be used for this purpose. Here we used DETMAX algorithm [18] which tries to find the best set of n measurements from a large database of random experiments. Hereafter, we refer to the selected set of conf-wrench combinations as Ψ. The following is the algorithm of finding the optimal set Ψ among the 875 conf-wrench combinations generated in the previous section:

(a) Randomly select n conf-wrench combinations from the 875 generated combinations and set them as the initial Ψ.

(b) Add each of the remaining $875-n$ conf-wrench combinations to Ψ, and calculate the observability index of the new $n+1$ combinations. Keep the conf-wrench combination which results in a greater observability index and add it to Ψ. Use the new Ψ with $n+1$ conf-wrench combinations in the next step.

(c) Remove one of the n+1 conf-wrench combinations of Ψ and calculate observability index of the new set. Execute this process for all the elements of Ψ, one by one, to find out removing of which combination will result in maximum observability index. Update Ψ by removing this conf-wrench combination. Therefore, the new Ψ consists of n conf-wrench combinations.

(d) Repeat steps (b) and (c) until the observability index of Ψ converges. This happens when the same conf-wrench combination added in step (b) is removed in step (c).

As it was mentioned, the minimum number of the conf-wrench combinations of Ψ for identifying the robot parameters is $m/3$ (i.e., $32/3 \simeq 11$ conf-wrench combinations); however, in our calibration process $n = 50$ conf-wrench combinations are used in order to reach more accurate results. With the optimal set of conf-wrench combinations and the corresponding measurements in hand, the robot parameters can be identified by the identification algorithm proposed in Section III.B. We used 0.05 mm as the stop criteria for this algorithm.

V. Experimental Setup

The experimental setup includes a FARO laser tracker, the 6-DOF cable-driven robot, the ABB 1600 serial robot, a 6-axis ATI force/torque sensor with its driver, a host PC, and a target PC. As it is shown in Fig. 5, the force sensor connects the moving platform of the cable-driven robot to the flange of the serial robot. This sensor measures the exact value of the wrench applied by the cable-driven robot on the end-effector of the ABB serial robot. The laser tracker is employed to measure the exact *xyz* position of the end-effector of the serial robot. To this end, the laser tracker target (SMR) is attached to the moving platform of the cable-driven robot. Deflections of the robot tool and the force sensor are negligible; therefore, we can suppose that the moving platform is rigidly connected to the serial robot flange. The cable-driven robot consists of a mobile platform and eight limbs. The limbs are made of cables. The length of each cable can be controlled by a cable winch mechanism. In order to be able to precisely control the forces applied by the cables to the mobile platform, we connected each cable to the mobile platform through an extension spring. The cable-driven robot has two degrees of redundancy. This redundancy is needed to provide 6D wrenches on the moving platform, in the presence of the physical constraint of positive forces in the cables. As the moving platform is a cube, several configurations are possible for connecting the cables to the vertices of the cube. The configuration which is used for this study is shown in Fig. 5.

In order to automatically perform the measurement procedure, the laser tracker, the ABB robot and the control hardware of the cable-driven robot are connected to a host computer through an Ethernet connection. The control hardware of the cable-driven robot consists of a real-time target PC which runs real-time codes provided by the xPC target toolbox of MATLAB. The real-time control codes are created by Simulink Coder and a C/C++ compiler in the host computer. The target PC is connected to the motor drivers via a Quanser Q8 data acquisition card which sends the control signals to the motors and reads the angular positions of the motors. This card also reads the analog data provided by the ATI six-channel force/torque sensor. The block diagram of the whole process is illustrated in Fig. 6.

While the ABB robot moves to a new position, the host computer reads the robot joint values and calculates the required cable lengths for the cable-driven robot at each instance. Therefore, the host computer is able to synchronize the movements of the cable-driven robot with the ABB robot. In order to calculate the required lengths of the cables, inverse kinematics equations of the cable-driven robot are solved at each step time. A force controller is implemented on the target PC in order to apply the desired wrench on the moving platform. Based on the feedback signals of the servo motor encoders and the force/torque sensor, the controller sends the required command to the servo motors to regulate the applied force on the robot end-effector. Using this experimental setup, a fully automated procedure is designed for the calibration experiment.

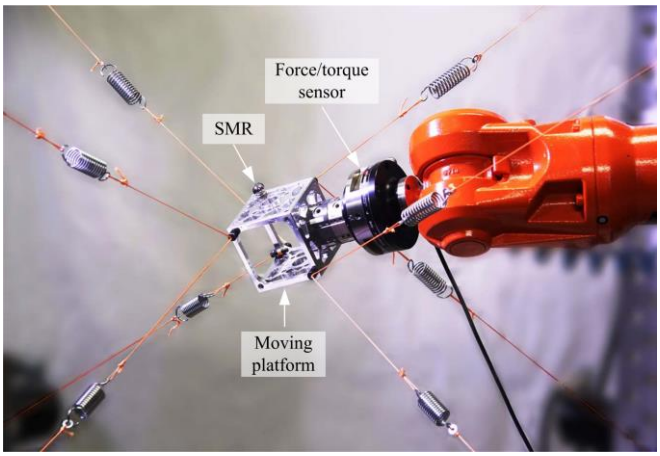

Figure 5. Connection of the moving platform of the cable-driven robot to the flange of the ABB robot

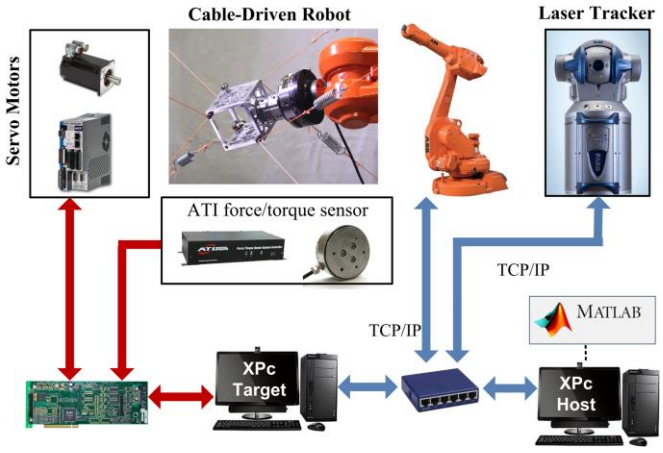

Figure 6. Hardware setup for control and measurement during the calibration process

The main program is developed in MATLAB and runs in the host PC. For each desired conf-wrench, first the program sends the required move command to the ABB robot to go to the desired robot configuration. Once the robot reaches the desired configuration, the host computer sends the desired wrench vector to the cable-driven robot controller (the target computer) and the force controller applies the required forces on the cables in order to apply the desired wrench on the moving platform. When the wrench is applied, the host computer solves the direct kinematics of the ABB robot with nominal parameters to obtain the approximate position of the end-effector. Laser tracker uses this estimated position to find the SMR. Next, it measures the precise position of the SMR and sends it to the host computer.

VI. Experiment Results

The proposed calibration experiment consists of two parts: calibration measurements, and validation measurements. All the 875 generated conf-wrenches in Section IV are used in our experiment. The 50 optimal conf-wrenches, which are selected in the Section IV.B, are used for the first set of measurements, dedicated to the parameter identification process. In the second set, the remaining 825 conf-wrench combinations are used for the validation measurements. The collected data of the calibration measurements is used for identifying the robot parameters. Both kinematic and elasto-geometrical calibrations are performed in order to compare the effect of the joint stiffness identification on the robot accuracy. The same robot configurations and external wrenches are used for the kinematic and elasto-geometrical calibration methods. The nominal calibration parameters and the identified parameters by the kinematic and elasto-geometrical methods are given in Table II.

In order to evaluate the calibration performance, the kinematic and elasto-geometrical models of the ABB robot is calculated for the second set of measurements (validation). The Euclidean norm of the position error is then calculated by the following equation:

$$e^k = \left\| \mathbf{x}_{\text{est}}^k - \mathbf{x}_{\text{measured}}^k \right\|, \tag{30}$$

TABLE II. The Nominal and Identified Robot Parameters

Parameters	*Nominal*	*Kinematic calibration*	*Elasto-geometrical calibration*
x_w (mm)	1326	1325.804	1327.583
y_w (mm)	1362	1362.859	1363.337
z_w (mm)	−1476	−1474.322	−1475.556
α_w (°)	−180	−180.209	−180.312
β_w (°)	0	0.512	0.494
γ_w (°)	0	−0.695	−0.596
x_t (mm)	22	23.582	22.193
y_t (mm)	50	49.193	50.024
z_t (mm)	150	148.973	148.905
$\delta\alpha_2$ (°)	0.000	−0.058	0.028
$\delta\alpha_3$ (°)	0.000	0.049	−0.011
$\delta\alpha_4$ (°)	0.000	−0.059	−0.009
$\delta\alpha_5$ (°)	0.000	0.092	−0.015
$\delta\alpha_6$ (°)	0.000	−0.025	0.092
δa_2 (mm)	0.000	1.519	0.971
δa_3 (mm)	0.000	−1.333	−1.017
δa_4 (mm)	0.000	−0.888	−0.804
δa_5 (mm)	0.000	0.052	0.122
δa_6 (mm)	0.000	−0.142	−0.067
δd_2 (mm)	0.000	−1.327	1.048
δd_4 (mm)	0.000	−2.592	−0.649
δd_5 (mm)	0.000	0.171	0.028
$\delta\theta_2$ (°)	0.000	−0.072	−0.069
$\delta\theta_3$ (°)	0.000	−0.080	−0.126
$\delta\theta_4$ (°)	0.000	0.008	−0.014
$\delta\theta_5$ (°)	0.000	−0.043	−0.032
k_1 (°/N.m)	0.000	n/a	0.00028
k_2 (°/N.m)	0.000	n/a	0.00023
k_3 (°/N.m)	0.000	n/a	0.00049
k_4 (°/N.m)	0.000	n/a	0.01126
k_5 (°/N.m)	0.000	n/a	0.01297
k_6 (°/N.m)	0.000	n/a	0.04147

where e^k is the position error of the k^{th} conf-wrench combination of the evaluation set. The measured position of the kth evaluation experiment is indicated by $\mathbf{x}_{\text{measured}}^k$ while $\mathbf{x}_{\text{est}}^k$ indicates the estimated position of the SMR calculated by calibration model. The joint values and external load of the kth conf-wrench combination and the identified error parameters are used in the calibration model. The error values are obtained for three different robot parameters: nominal, identified by kinematic calibration and identified by the proposed elasto-geometrical calibration method. For each set of parameters, the position errors for the validation set of conf-wrench combinations are calculated.

Results are summarized in Table III and Fig. 7. They show that the maximum position error of the ABB robot is decreased from 5.954 mm before calibration to 0.960 mm af-

ter elasto-geometrical calibration. The kinematic calibration of the robot under the same conf-wrenches reduced the maximum error to only 2.571 mm. The median and standard deviation of the errors also confirm that the robot accuracy improved significantly after the proposed elasto-geometrical calibration. Statistical significance was tested using two-tailed Student's t-test analysis on the positioning error. Results reveal significant differences between the positioning errors after the kinematic calibration and elasto-geometrical calibration (p-value $\ll 0.05$). Evaluation results confirm that using the optimal model parameters in the proposed elasto-geometrical calibration model, a more accurate end-effector position can be obtained in comparison with the kinematic calibration.

VII. Conclusion

We presented a new method for elasto-geometrical calibration of industrial robots. Using a cable-driven robot, multi-directional forces and torques were applied to the end-effector of an industrial robot in order to identify the stiffness parameters of its joints. A total of 875 combinations of robot configuration and end-effector wrench are generated for the experiment from which 50 were selected based on an observability analysis. The experimental calibration was performed for the 50 selected combinations and the results were validated by the remaining 825 combinations. In order to assess the efficiency of the proposed elasto-geometrical calibration, accuracy of the robot in the presence of the external loads were compared for three different robot parameters: (1) nominal values; (2) identified by kinematic calibration; (3) identified by elasto-geometrical calibration. Results show that when the industrial robot's end-effector is under external loads, the kinematic calibration cannot make a significant improvement in the robot accuracy. However, the proposed elasto-geometrical calibration reduces the position errors by a large factor.

TABLE III. Position errors before and after calibration

	Nominal	*Kinematic calibration*	*Elasto-geometrical calibration*
Mean	2.486	0.943	0.264
Std.	1.745	0.479	0.137
Max	5.954	2.571	0.960

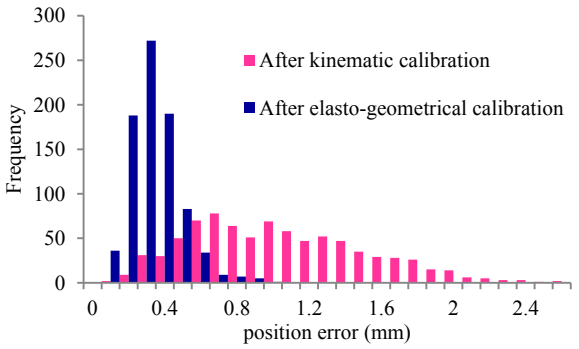

Figure 7. Histogram of the ABB robot position errors after kinematic calibration and after the proposed elasto-geometrical calibration

References

[1] Z. S. Roth, B. W. Mooring, and B. Ravani, "An overview of robot calibration," *IEEE J. Robot. Automat.*, vol. 3, no. 5, pp. 377–385, 1987.

[2] A. Y. Elatta, L. P. Gen, F. L. Zhi, Y. Daoyuan, and L. Fei, "An overview of robot calibration," *Inform. Technol. J.*, vol. 3, no. 1, pp. 74–78, 2004.

[3] J.-M. Renders, E. Rossignol, M. Becquet, and R. Hanus, "Kinematic calibration and geometrical parameter identification for robots," *IEEE Trans. Robot. Automat.*, vol. 7, no 6, pp 721–732, 1991.

[4] H. Shi, H.-J Su, N. Dagalakis, and J. A. Kramar, "Kinematic modeling and calibration of a flexure based hexapod nanopositioner," *Precision Eng.*, vol. 37, no. 1, pp. 117–128, 2013.

[5] A. Joubair, and I. A. Bonev. "Kinematic calibration of a six-axis serial robot using distance and sphere constraints," *Int. J. Adv. Manuf. Technol.*, vol. 77, no. 1-4, pp. 515–523, 2015.

[6] A. Joubair, and I. A. Bonev, "Non-kinematic calibration of a six-axis serial robot using planar constraints," *Precision Eng.*, vol. 40, pp. 325–333, 2015.

[7] J. Zhou, H.-N. Nguyen, and H.-J. K, "Simultaneous identification of joint compliance and kinematic parameters of industrial robots," *Int. J. Precision Eng. Manufact*., vol. 15, no. 11, pp. 2257–2264, 2014.

[8] Y. Wu, A. Klimchik, S. Caro, C. Boutolleau, B. Furet, and A. Pashkevich, "Experimental study on geometric and elastostatic calibration of industrial robot for milling application," in *Proc. 2014 IEEE/ASME Int. Conf. Advanced Intelligent Mechatronics*, Besançon, France, pp. 1688–1696, 2014.

[9] S. Marie, E. Courteille, and P. Maurine, "Elasto-geometrical modeling and calibration of robot manipulators: Application to machining and forming applications," *Mechanism and Machine Theory*, vol. 69, pp. 13-43, 2013.

[10] J. Wang, H. Zhang, and T. Fuhlbrigge, "Improving machining accuracy with robot deformation compensation," in *Proc. IROS 2009 IEEE/RSJ Int. Conf. Intelligent Robots and Systems*, St. Louis, MO, pp. 3826–3830, 2009.

[11] A. Joubair, A. Nubiola, and I. A. Bonev, "Calibration efficiency analysis based on five observability indices and two calibration models for a six-axis industrial robot," *SAE Int. J. Aerosp.*, vol. 6, no. 1, pp. 161–168, 2013.

[12] A. Nubiola, and I. A. Bonev, "Absolute calibration of an ABB IRB 1600 robot using a laser tracker," *Robotics and Computer-Integrated Manufacturing*, vol. 29, no.1, pp. 236-245, 2013.

[13] M. Gouttefarde, and C. M. Gosselin, "Analysis of the Wrench-Closure Workspace of Planar Parallel Cable-Driven Mechanisms," *IEEE Trans. Robotics*, vol. 22, no. 3, pp. 434-445, 2006.

[14] J. J. Craig, *Introduction to robotics: mechanics and control,* 3rd ed. Upper Saddle River: Pearson Prentice Hall, 2005.

[15] A. Joubair, I. A. Bonev, "Comparison of the efficiency of five observability indices for robot calibration," *Mechanism and Machine Theory*, vol. 70, pp. 254-265, 2013.

[16] Y. Sun, and J. M. Hollerbach, "Observability index selection for robot calibration," in *Proc. IEEE international conference on robotics and automation*, Pasadena, CA, pp. 831–836, 2008.

[17] A. Joubair, L. F. Zhao, P. Bigras, and I. Bonev, "Absolute accuracy analysis and improvement of a hybrid 6-DOF medical robot," *Industrial Robot: An International Journal*, vol.42, no. 1, pp. 44-53, 2015.

[18] T. J. Mitchell, "An algorithm for the construction of D-optimal experimental designs," *Technometrics*, vol. 16, no. 2, pp. 203–210, 1974.